NASA Technical Memorandum 101607

PRELIMINARY INVESTIGATION OF PARAMETER SENSITIVITIES FOR ATMOSPHERIC ENTRY AND AEROBRAKING AT MARS

(NASA-TM-101607) PRELIMINARY INVESTIGATION OF PARAMETER SENSITIVITIES FOR ATMOSPHERIC ENTRY AND AEROBRAKING AT MARS (NASA) 30 p N90-17667
CSCL 22B Unclas
G3/18 0253006

Mary C. Lee and
William T. Suit

September 1989

National Aeronautics and
Space Administration

Langley Research Center
Hampton, Virginia 23665-5225

ABSTRACT

The proposed manned Mars mission will need to be as weight efficient as possible. This paper will discuss one way of lowering the weight of the vehicle by using aeroassist braking instead of retro-rockets to slow a craft once it reaches its destination. The two vehicles studied are a small vehicle similar in size to the Mars Rover Sample Return (MRSR) vehicle and a larger vehicle similar in size to a six person Manned Mars Mission (MMM) vehicle. Simulated entries were made using various coefficients of lift (C_L), coefficients of drag (C_D), and lift-to-drag ratios (L/D). A range of acceptable flight path angles with their corresponding bank angle profiles was found for each case studied. These ranges were then compared, and the results are reported here. The sensitivity of velocity and acceleration to changes in flight path angle and bank angle is also included to indicate potential problem areas for guidance and navigation system design.

INTRODUCTION

In anticipation of a manned Mars mission as well as a Mars sample return mission, there has been much research done and many papers written on aeroassist braking in the Earth's atmosphere (reference 1). However, the return to Earth is only half of the trip. First, we must get to Mars and achieve an orbit there. In order to save valuable weight, aeroassist braking will be used to slow the craft at Mars, just as it will at Earth.

Aeroassist braking involves using the atmosphere of a planet to decelerate a craft instead of using retro-rockets. The craft enters the atmosphere and uses the air particles to deplete its kinetic energy, slowing the craft to a velocity that will allow orbital capture (reference 2).

The actual configuration for the aerobrake for a manned Mars mission is still being investigated, so a range of possible vehicles was considered. Within the range of ballistic coefficients covered in the paper a range of aerobrake sizes, weights, and L/D ratios were considered. The purpose of this paper is to present the results of a Mars entry study using various combinations of vehicle parameters. The study will present combinations of initial flight path angles and bank angles required for capture at Mars. Entry windows and relative sensitivities for various vehicle combinations will also be shown.

SYMBOLS

A	vehicle reference area, square meters
ASM	acceleration, meters/sec/sec
C_D	drag coefficient
C_L	lift coefficient
hp_1	first pass perigee altitude, nautical miles
hp_2	second pass perigee altitude, nautical miles
L/D	lift-to-drag ratio
M	mass, kilograms
V_I	inertial velocity, meters/sec

ϕ	bank angle, degrees
γ_I	initial flight path angle, degrees
ΔV	change in velocity, meters/sec

SYMBOLS FOR FIGURES

ALTITO	altitude, meters
ASMG	acceleration, "g" units
BNKANG	bank angle, degrees
VELI	velocity, meters/sec

APPROACH

The studies conducted in this paper were made using a software package known as the Program to Optimize Simulated Trajectories (POST). This program can be used to determine initial parameters and control parameters throughout a trajectory to accomplish stated mission objectives. For this study, all simulated entries consist of three steps, regardless of vehicle size or L/D ratio. First, the vehicle enters the atmosphere at 300 km with an entry flight path angle determined by POST. The aerodynamic forces on the vehicle are small until 125 km, however, atmospheric data were available up to 300 km and so the problem was started there. Next, the program calculates a set of bank angles that should result in capture. Third, the craft's final trajectory is achieved. This trajectory can be hyperbolic, elliptical with eventual impact, elliptical with capture, or impact on the first pass. The trajectories discussed here are either elliptical with eventual impact or elliptical with capture. Eventual impact means that the program predicted impact on the second pass, but achieved capture on the first pass. To correct this problem of impact, slight thrust can be added at some point in the trajectory to give the needed boost to a higher orbit. This is another point for additional study and will not be discussed to any great extent within this paper.

It can be observed that the individual bank angles that result in capture do not occur at regular time intervals. The intervals were determined by looking at plots of the profiles and decreasing the number of data points by combining adjacent times that showed little to no change compared with one another.

A vehicle smaller than those proposed for a manned Mars mission was used in the beginning of the study for two reasons. First, to confirm that the program would run correctly, data from the program were checked with data available from other sources. (The second reason was to gather data that might be used for a lander vehicle deployed from the larger manned vehicle.) The physical and aerodynamic characteristics used for the small vehicle are given in Table 1. Runs were made for L/D equal to 1.5, 1.0, and .5 with $C_D = 2$.

Once the smaller vehicle runs were completed, a larger vehicle representative of a manned Mars mission (MMM) vehicle which could carry a crew of five to seven members and the supplies needed for the mission was investigated. Two "large" vehicles were considered. The physical and aerodynamic characteristics of the large vehicle are presented in Table 2. The first runs of the MMM vehicle were made with an L/D of 1.0 where $C_L = C_D = 2$. Then, the C_L was changed to 1 as with the small vehicle, and runs with L/D = 0.5 were made.

Since the Viking probes returned their data on the Martian atmosphere, several different atmosphere models have been developed. For the runs described above, one of these atmospheres (atmosphere 1) was chosen and put into tables that were suitable to the program (Table 3). Near the end of the project time, when the runs with atmosphere 1 were completed, a second atmosphere (atmosphere 2) was tabulated and introduced into the program. The purpose of this switch was to determine if there was any significant change in the acceptable flight path angle windows from those determined using atmosphere 1.

RESULTS AND DISCUSSION

Initially Mars entry runs were made trying to achieve capture with a single fixed bank angle. The problem was extremely sensitive to changes in initial flight path angle and bank angle and no combination of the two angles was found that would result in capture. Changes of the order of .0001° would result in either impact or skip-out. At this point, the multiple bank angle approach was tried. The problem was split into time slots and POST was asked to select the bank angles that would result in a capture trajectory. The entry flight path angle and bank angles are given in Table 4 .

To determine the flight-path-angle window that would result in capture, two sets of runs were made: one set to determine the least negative entry flight path angle and a second set to determine the most negative flight path angle possible. The difference in these entry-flight-path angles gave the entry-flight-path-angle window.

For each of these maximum and minimum flight path angles, a bank angle profile that would result in capture was determined for every vehicle. In addition to ensuring capture, these runs had perigee altitudes greater than 30 km. In all of the maximum initial flight path angle (least negative) cases and in many of the minimum flight path angle (most negative) cases the second pass orbit also would have an acceptable perigee altitude. The results of these runs are given in Table 4 and typical time histories are shown in figures 1 and 2. Generally, the maximum flight path angle runs stayed higher in the atmosphere and remained in the atmosphere for longer periods of time than the minimum flight path angle runs which plunged deeper into the atmosphere and usually reached their minimum altitude within the first 200 seconds of the run (figure 2). From Table 4 and figure 1, the bank angles for the maximum flight path angle runs are seen to tend toward lift down (full lift down = 180°) in order to keep the craft in the dense atmosphere long enough to decelerate to capture velocity. Conversely, the minimum flight path angle runs tended toward lift up (full lift up=0°) to pull the craft out of the more dense atmosphere before too much energy was lost, causing the craft to crash into the planet's surface.

In general for the vehicles investigated the entry flight path window was about 1.5° (figure 3). At larger L/D's the vehicles with a smaller M/C_D*A tended to have a slightly smaller window (Table 4), while at L/D=.5 no significant effect of M/C_D*A was seen. Also, for a given M/C_D*A the entries had a greater energy loss as L/D decreased. The perigee altitudes showed no consistent trends with L/D or M/C_D*A. However, the bank angle profiles were affected by changes in both M/C_D*A and L/D (figures 1 & 2). The changes were especially noticeable with the minimum flight path angle runs (figure 1 & Table 4). Maximum flight path angle entries using vehicles with higher L/D ratios and larger M/C_D*A values tended to deviate more from full lift down and these trends were stronger with L/D ratios of .5 where the entries were predominantly lift down throughout the run (figure 1 & Table 4). The significant point from these runs was that, given a 1/2° window in the middle of the extremes, a set of bank angles could be found so that capture was possible. This implies that the entry corridor is wide enough so that guidance systems that would result in capture can be designed for the range of vehicles considered in this study.

Table 5 shows the sensitivity of various trajectory parameters to changes in flight path angle for a given set of bank angles. The sensitivities were not shown for all runs since the trends and values seen can be illustrated using the tables given. The table shows that if the bank angles are fixed for a particular entry trajectory then very small variations of entry flight path angle have a significant effect on the trajectory. A second observation is that the types of trajectories flown can influence the sensitivity to entry flight path angle. Trajectories that stayed higher in the atmosphere during the initial part of the entry tended to be more sensitive to changes in initial flight path angle than those trajectories that initially penetrated deeper into the atmosphere. The implication is that for a fixed bank angle sequence the entry/capture trajectory was more sensitive to changes in initial flight path angle error when the braking was over a longer duration than was true for trajectories that flew higher in the atmosphere. The message for designers of guidance systems is that braking higher in the atmosphere where "g" loads are less and heating is less could require more precise guidance systems. This problem must be examined further.

Table 5 also shows the sensitivity of various trajectory parameters to the different bank angles in the bank angle sequence. As expected the greatest sensitivity occurred when the vehicle was deepest in the atmosphere and the forces on the vehicle were greatest (figure 1 & Table 5). In most cases the trajectory parameters were not particularly sensitive to bank angle changes. However, since the minimum altitude ,"g" load, and heat rate could be altered by changing the bank angles, further investigation of the effect of the problem formulation on the bank angle sequence should be conducted.

To determine the effect of flying through a different Martian atmosphere runs were made using a second atmospheric model. Atmosphere 2 is given in Table 3 and was used during the design of the Viking lander. Data received from Viking indicated that this atmosphere was close to that of Mars at several altitudes. To examine the effect of another atmosphere, small vehicle 2 and large vehicle 2 were used. Both vehicles were assumed to have an L/D = 1 and $C_D = 2$. The results are shown in Tables 6 & 7 and figure 4. The initial flight-path-angle window and the sensitivities were similar to those seen with the previous atmosphere. For the maximum flight path angle runs, the initial bank angle runs were different since atmosphere 2 was more dense at higher altitudes (figure 4). However, the altitude profile was not significantly different when the vehicle flew through atmosphere 2.

CONCLUSIONS

For the vehicles investigated, entry flight-path-angle windows in excess of 1° were found. This included vehicles with a M/C_D*A (representative of a six-person Mars mission vehicle) with a 15.24 m (50 ft) diameter aeroshell. While this window should offer a reasonable target for a Martian aerocapture, the study also indicated that the capture trajectories were very sensitive to errors in the entry flight path angle. Trajectories flying higher in the atmosphere seemed to have a greater sensitivity to errors than those flying lower in the atmosphere. As expected, the sensitivity to bank angle error was greatest in the region where the aerodynamic forces were greatest. However, the projected state errors were not so large as to imply that a bank angle guidance/control system could not be flown.

A limited number of runs were made with a second model of the Martian atmosphere. These runs showed only minimal differences from those runs made using the original atmospheric model.

SUGGESTED STUDIES

1. The current study looked at vehicles with four different ballistic coefficients (M/C_D*A). However, these vehicles all had the same drag coefficient and were scaled to meet various weight or L/D combinations. Other vehicle types, blunter or more streamlined, should be investigated.

2. Only two Martian atmospheres were considered, one of these for only a limited number of runs. Additional atmospheric models need to be included in future studies.

3. One check on the ΔV required to get an acceptable second pass orbit was made. The ΔV required to get an acceptable second pass was small and similar calculations need to be made for any runs that did not have an acceptable second pass orbit.

REFERENCES

1. Walberg, Gerald D.: A Review of Aeroassisted Orbital Transfer. AIAA Paper No. 82-1378, AIAA 9th Atmospheric Flight Mechanics Conference, San Diego , CA , August 1982.

2. Walberg, Gerald D.: A Review of Aerobraking for Mars Missions. IAF Paper No. IAF-88-196, 39th Congress of the International Astronautical Federation, Bangalore, India , October 1988.

TABLE 1 VEHICLE CHARACTERISTICS

SMALL VEHICLE

Vehicle 1 $\frac{M}{C_D A} = 500 \frac{kg}{m^2}$, $A = 16\ m^2$, $C_D = 2$

$M = 16{,}000$ kg

Vehicle 2 $\frac{M}{C_D A} = 1{,}000 \frac{kg}{m^2}$, $A = 16\ m^2$, $C_D = 2$

$M = 32{,}000$ kg

TABLE 2 VEHICLE CHARACTERISTICS

LARGE VEHICLE

Vehicle 1 $\frac{M}{C_D A} = 622 \frac{kg}{m^2}$, $A = 182\ m^2$, $C_D = 2$

$M = 226{,}378$ kg

Vehicle 2 $\frac{M}{C_D A} = 1{,}147 \frac{kg}{m^2}$, $A = 182\ m^2$, $C_D = 2$

$M = 417{,}560$ kg

TABLE 3 ATMOSPHERIC DENSITIES FOR MARS

ATMOSPHERE 1

Altitude, m	Density kg/m^3	Altitude, m	Density kg/m^3	Altitude, m	Density kg/m^3	Altitude, m	Density kg/m^3
0	1.55E-02	50,000	1.08E-04	100,000	1.59E-07	200,000	5.15E-12
5000	9.91E-03	55,000	5.92E-05	110,000	4.4E-08	210,000	2.43E-12
10,000	6.47E-03	60,000	3.19E-05	120,000	1.0E-08	220,000	1.15E-12
15,000	4.17E-03	65,000	1.68E-05	130,000	2.62E-09	230,000	5.48E-13
20,000	2.63E-03	70,000	8.73E-06	140,000	7.89E-10	240,000	2.62E-13
25,000	1.62E-03	75,000	4.48E-06	150,000	2.72E-10	250,000	1.26E-13
30,000	9.8E-04	80,000	2.29E-06	160,000	1.2E-10	260,000	6.05E-14
35,000	5.82E-04	85,000	1.17E-06	170,000	5.37E-11	270,000	2.93E-14
40,000	3.4E-04	90,000	6.02E-07	180,000	2.43E-11	280,000	1.42E-14
45,000	1.94E-04	95,000	3.09E-07	190,000	1.11E-11	290,000	6.93E-15
						300,000	3.39E-15

ATMOSPHERE 2

Altitude, m	Density kg/m^3	Altitude, m	Density kg/m^3	Altitude, m	Density kg/m^3	Altitude, m	Density kg/m^3
0	7.56E-03	75,000	1.14E-05	150,000	9.02E-08	225,000	8.54E-09
5000	5.72E-03	80,000	6.79E-06	155,000	7.41E-08	230,000	7.76E-09
10,000	4.11E-03	85,000	4.24E-06	160,000	6.13E-08	235,000	7.05E-09
15,000	2.80E-03	90,000	2.75E-06	165,000	5.06E-08	240,000	6.41E-09
20,000	1.90E-03	95,000	1.83E-06	170,000	4.19E-08	245,000	5.85E-09
25,000	1.27E-03	100,000	1.25E-06	175,000	3.48E-08	250,000	5.34E-09
30,000	8.42E-04	105,000	8.80E-07	180,000	2.91E-08	255,000	4.92E-09
35,000	5.52E-04	110,000	6.33E-07	185,000	2.43E-08	260,000	4.53E-09
40,000	3.59E-04	115,000	4.64E-07	190,000	2.04E-08	265,000	4.23E-09
45,000	2.30E-04	120,000	3.47E-07	195,000	1.72E-08	270,000	3.94E-09
50,000	1.46E-04	125,000	2.63E-07	200,000	1.45E-08	275,000	3.68E-09
55,000	8.97E-05	130,000	2.03E-07	205,000	1.29E-08	280,000	3.34E-09
60,000	5.45E-05	135,000	1.65E-07	210,000	1.16E-08	285,000	3.20E-09
65,000	3.32E-05	140,000	1.35E-07	215,000	1.04E-08	290,000	2.99E-09
70,000	2.02E-05	145,000	1.10E-07	220,000	9.43E-09	295,000	2.79E-09
						300,000	2.61E-09

TABLE 4 BANK ANGLES FOR VARIOUS VEHICLES AND INITIAL FLIGHT PATH ANGLES

SMALL VEHICLE 1

L/D	C_L	C_D	M/C_DA
1.5	3.0	2.0	500

MAXIMUM FLIGHT PATH ANGLE

$hp_1 = 40.0$ nm $hp_2 = 50.77$ nm $\gamma_I = -18.10$ deg

TIME	0 TO 197	197 TO 225	225 TO 240	240 TO 250	250 TO 270	270 TO 280	280 TO 293	293 TO END
ϕ, deg	128	134	99	90	71	62	60	180

MINIMUM FLIGHT PATH ANGLE

$hp_1 = 41.8$ nm $hp_2 = 63.3$ nm $\gamma_I = -19.45$ deg

TIME	0 TO 197	197 TO 225	225 TO 240	240 TO 250	250 TO 270	270 TO 280	280 TO 293	293 TO 305	305 TO END
ϕ, deg	63.4	265	142	137.5	102.1	69.9	63.5	184.5	180

SMALL VEHICLE 1

L/D	C_L	C_D	M/C_DA
1.0	2.0	2.0	500

MAXIMUM FLIGHT PATH ANGLE

$hp_1 = 46.1$ nm $hp_2 = 62.4$ nm $\gamma_I = -18.06$ deg

TIME	0 TO 197	197 TO 225	225 TO 240	240 TO 250	250 TO 270	270 TO 280	280 TO 293	293 TO 305	305 TO END
ϕ, deg	258.4	199	111	115	98	75	68	193	180

MINIMUM FLIGHT PATH ANGLE

$hp_1 = 38.5$ nm $hp_2 = 11$ nm $\gamma_I = -19.35$ deg

TIME	0 TO 197	197 TO 225	225 TO 240	240 TO 250	250 TO 270	270 TO 280	280 TO 293	293 TO END
ϕ, deg	70	73	49	52	57	60	60	180

TABLE 4 BANK ANGLES FOR VARIOUS VEHICLES AND INITIAL FLIGHT PATH ANGLES (CONTINUED)

SMALL VEHICLE 1

L/D	C_L	C_D	M/C_DA
.5	1.0	2.0	500

MAXIMUM FLIGHT PATH ANGLE

$hp_1 = 43.0$ nm $hp_2 = 50.9$ nm $\gamma_I = -18.2$ deg

TIME	0 TO 197	197 TO 225	225 TO 240	240 TO 250	250 TO 270	270 TO 280	280 TO 293	293 TO 305	305 TO END
ϕ, deg	178.4	189.2	98.6	95.6	80.6	66.8	63.5	185.7	180

MINIMUM FLIGHT PATH ANGLE

$hp_1 = 37.5$ nm $hp_2 = 4.43$ nm $\gamma_I = -19.52$ deg

TIME	0 TO 197	197 TO 225	225 TO 240	240 TO 250	250 TO 270	270 TO 280	280 TO 293	293 TO 305	305 TO END
ϕ, deg	.7	6.6	50	56	58	60	60	179	180

SMALL VEHICLE 2

L/D	C_L	C_D	M/C_DA
1.5	3.0	2.0	1000

MAXIMUM FLIGHT PATH ANGLE

$hp_1 = 36.5$ nm $hp_2 = 59.9$ nm $\gamma_I = -18.17$ deg

TIME	0 TO 197	197 TO 225	225 TO 240	240 TO 250	250 TO 270	270 TO 280	280 TO 293	293 TO 305	305 TO END
ϕ, deg	187.4	147	102	103	78	65	62	183	180

MINIMUM FLIGHT PATH ANGLE

$hp_1 = 34.86$ nm $hp_2 = 25.05$ nm $\gamma_I = -19.75$ deg

TIME	0 TO 197	197 TO 225	225 TO 240	240 TO 250	250 TO 270	270 TO 280	280 TO 293	293 TO END
ϕ, deg	64	258	53	50	58	60	60	180

TABLE 4 BANK ANGLES FOR VARIOUS VEHICLES AND INITIAL FLIGHT PATH ANGLES (CONTINUED)

SMALL VEHICLE 2

L/D	C_L	C_D	M/C_DA
1	2.0	2.0	1000

MAXIMUM FLIGHT PATH ANGLE

$hp_1 = 37.7$ nm $hp_2 = 56.0$ nm $\gamma_I = -18.24$deg

TIME	0 TO 197	197 TO 225	225 TO 240	240 TO 250	250 TO 270	270 TO 280	280 TO 293	293 TO 305	305 TO END
φ, deg	191	191	100	101	85	69	64	187	180

MINIMUM FLIGHT PATH ANGLE

$hp_1 = 32.5$ nm $hp_2 = 33.7$ nm $\gamma_I = -19.9$ deg

TIME	0 TO 197	197 TO 225	225 TO 240	240 TO 250	250 TO 270	270 TO 280	280 TO 293	293 TO 305
φ, deg	52	272	72	66	61	60	60	180

SMALL VEHICLE 2

L/D	C_L	C_D	M/C_DA
.5	1.0	2.0	1000

MAXIMUM FLIGHT PATH ANGLE

$hp_1 = 40.2$nm $hp_2 = 50.2$ nm $\gamma_I = -18.34$ deg

TIME	0 TO 197	197 TO 225	225 TO 240	240 TO 250	250 TO 270	270 TO 280	280 TO 293	293 TO 305	305 TO END
φ, deg	145	189	163	177	141	92	79	202	180

MINIMUM FLIGHT PATH ANGLE

$hp_1 = 30.8$ nm $hp_2 = -5.3$ nm $\gamma_I = -19.79$ deg

TIME	0 TO 197	197 TO 225	225 TO 240	240 TO 250	250 TO 270	270 TO 280	280 TO 293	293 TO END	305 TO END
φ, deg	.7	7.0	49	5.6	58	59	60	179	180

TABLE 4 BANK ANGLES FOR VARIOUS VEHICLES AND INITIAL FLIGHT PATH ANGLES (CONTINUED)

LARGE VEHICLE 1

L/D	C_L	C_D	M/C_DA
1	2.0	2.0	622

MAXIMUM FLIGHT PATH ANGLE

hp_1 = 42.7 nm hp_2 = 60.5 nm γ_1 = -18.06 deg

TIME	0 TO 197	197 TO 225	225 TO 240	240 TO 250	250 TO 270	270 TO 280	280 TO 293	293 TO 305	305 TO END
ϕ, deg	193.6	194.6	110	110	88.3	68.5	64.4	185.4	180

MINIMUM FLIGHT PATH ANGLE

hp_1 = 36.8 nm hp_2 = 17 nm γ_1 = -19.5 deg

TIME	0 TO 197	197 TO 225	225 TO 240	240 TO 250	250 TO 270	270 TO 280	280 TO 293	293 TO 305	305 TO END
ϕ, deg	66	97	45	47	55	59	60	179	180

LARGE VEHICLE 1

L/D	C_L	C_D	M/C_DA
.5	1.0	2.0	622

MAXIMUM FLIGHT PATH ANGLE

hp_1 = 43.1nm hp_2 = 52.9 nm γ_1 = -18.2 deg

TIME	0 TO 197	197 TO 225	225 TO 240	240 TO 250	250 TO 270	270 TO 280	280 TO 293	293 TO 305	305 TO END
ϕ, deg	211	191	124	127	106	79	71	196	180

MINIMUM FLIGHT PATH ANGLE

hp_1 = 34.0 nm hp_2 = -8.4 nm γ_1 = -19.8 deg

TIME	0 TO 197	197 TO 225	225 TO 240	240 TO 250	250 TO 270	270 TO 280	280 TO 293	293 TO END	305 TO END
ϕ, deg	-.4	16	53	56	58	60	60	179	180

TABLE 4 BANK ANGLES FOR VARIOUS VEHICLES AND INITIAL FLIGHT PATH ANGLES (CONCLUDED)

LARGE VEHICLE 2

L/D	C_L	C_D	M/C_DA
1	2.0	2.0	1147

MAXIMUM FLIGHT PATH ANGLE

$hp_1 = 39.4$ nm $hp_2 = 55.6$ nm $\gamma_1 = -18.33$ deg

TIME	0 TO 197	197 TO 225	225 TO 240	240 TO 250	250 TO 270	270 TO 280	280 TO 293	293 TO 305	305 TO END
ϕ, deg	113	182	111	118	100	76	69	194	180

MINIMUM FLIGHT PATH ANGLE

$hp_1 = 31.3$ nm $hp_2 = 32.1$ nm $\gamma_1 = -19.97$ deg

TIME	0 TO 197	197 TO 225	225 TO 240	240 TO 250	250 TO 270	270 TO 280	280 TO 293	293 TO 305	305 TO END
ϕ, deg	51	277	71	65	61	60	60	60	180

LARGE VEHICLE 2

L/D	C_L	C_D	M/C_DA
.5	1.0	2.0	1147

MAXIMUM FLIGHT PATH ANGLE

$hp_1 = 37.8$ nm $hp_2 = 48.9$ nm $\gamma_1 = -18.41$ deg

TIME	0 TO 197	197 TO 225	225 TO 240	240 TO 250	250 TO 270	270 TO 280	280 TO 293	293 TO 305	305 TO END
ϕ, deg	219	192	129	135	113	83	7.4	199	180

MINIMUM FLIGHT PATH ANGLE

$hp_1 = 28.07$ nm $hp_2 = -12.7$ nm $\gamma_1 = -20.02$ deg

TIME	0 TO 197	197 TO 225	225 TO 240	240 TO 250	250 TO 270	270 TO 280	280 TO 293	293 TO END	305 TO END
ϕ, deg	-2.4	46	53	56	58	60	60	179	180

TABLE 5 SENSITIVITIES TO VARIATION IN INITIAL FLIGHT PATH ANGLE AND BANK ANGLE FOR VARIOUS VEHICLES

SMALL VEHICLE 2

L/D	C_L	C_D	M/C_DA
1.5	3	2	1000

MAXIMUM FLIGHT PATH ANGLE

$\Delta V_I/\Delta\gamma_I = 2.45$ E4 M/S/DEG $\Delta ASM/\Delta\gamma_I = -129.6$ $M/sec^2/DEG$

TIME,SEC	0 TO 197	197 TO 225	225 TO 240	240 TO 250	250 TO 270	270 TO 280	280 TO 293	293 TO 305	305 TO END
$\Delta V_I/\Delta\phi$	-25	-67	-86	-129	-142	-86	-56	-10	0
$\Delta ASM/\Delta\phi$	.13	.33	.38	.36	.12	0	0	0	0

MINIMUM FLIGHT PATH ANGLE

$\Delta V_I/\Delta\gamma_I = -1.97$ E3 M/S/DEG $\Delta ASM/\Delta\gamma_I = -37.2$ $M/sec^2/DEG$

TIME,SEC	0 TO 197	197 TO 225	225 TO 240	240 TO 250	250 TO 270	270 TO 280	280 TO 293	293 TO 305	305 TO END
$\Delta V_I/\Delta\phi$	-134.3	-2.3	-2.0	-1.6	-.6	0	0	0	0
$\Delta ASM/\Delta\phi$	.83	0	0	0	0	0	0	0	0

SMALL VEHICLE 2

L/D	C_L	C_D	M/C_DA
1	2	2	1000

MAXIMUM FLIGHT PATH ANGLE

$\Delta V_I/\Delta\gamma_I = -1.42$ E4 M/S/DEG $\Delta ASM/\Delta\gamma_I = -257$ $M/sec^2/DEG$

TIME,SEC	0 TO 197	197 TO 225	225 TO 240	240 TO 250	250 TO 270	270 TO 280	280 TO 293	293 TO 305	305 TO END
$\Delta V_I/\Delta\phi$	4	10	-36	-50	-46	-25	-16	-3	0
$\Delta ASM/\Delta\phi$	0	0	.18	.17	0	0	0	0	0

MINIMUM FLIGHT PATH ANGLE

$\Delta V_I/\Delta\gamma_I = -4.15$ E3 M/S/DEG $\Delta ASM/\Delta\gamma_I = -27$ $M/sec^2/DEG$

TIME,SEC	0 TO 197	197 TO 225	225 TO 240	240 TO 250	250 TO 270	270 TO 280	280 TO 293	293 TO 305	305 TO END
$\Delta V_I/\Delta\phi$	-56	-.16	-.4	-.25	0	0	0	0	0
$\Delta ASM/\Delta\phi$	.31	0	0	0	0	0	0	0	0

TABLE 5 SENSITIVITIES TO VARIATION IN INITIAL FLIGHT PATH ANGLE AND BANK ANGLE FOR VARIOUS VEHICLES (CONTINUED)

SMALL VEHICLE 2

L/D	C_L	C_D	M/C_DA
.5	1	2	1000

MAXIMUM FLIGHT PATH ANGLE

$\Delta V_I/\Delta\gamma_I$ = 1.013 E4 M/S/DEG $\Delta ASM/\Delta\gamma_I$ = -153 $M/sec^2/DEG$

TIME,SEC	0 TO 197	197 TO 225	225 TO 240	240 TO 250	250 TO 270	270 TO 280	280 TO 293	293 TO 305	305 TO END
$\Delta V_I/\Delta\phi$	-19.5	-4.4	-13.9	-16.8	-14.4	-8	-5.4	-.6	0
$\Delta ASM/\Delta\phi$	0	0	0	0	0	0	0	0	0

MINIMUM FLIGHT PATH ANGLE

$\Delta V_I/\Delta\gamma_I$ = 971 E3 M/S/DEG $\Delta ASM/\Delta\gamma_I$ = -24 $M/sec^2/DEG$

TIME,SEC	0 TO 197	197 TO 225	225 TO 240	240 TO 250	250 TO 270	270 TO 280	280 TO 293	293 TO 305	305 TO END
$\Delta V_I/\Delta\phi$	-.56	-.61	0	0	0	0	0	0	0
$\Delta ASM/\Delta\phi$	0	0	0	0	0	0	0	0	0

TABLE 5 SENSITIVITIES TO VARIATION IN INITIAL FLIGHT PATH ANGLE AND BANK ANGLE FOR VARIOUS VEHICLES (CONTINUED)

LARGE VEHICLE 2

L/D	C_L	C_D	M/C_DA
1	2	2	1147

MAXIMUM FLIGHT PATH ANGLE

$\Delta V_I/\Delta\gamma_I = -1.37$ E4 M/S/DEG $\Delta ASM/\Delta\gamma_I = -229$ $M/sec^2/DEG$

TIME,SEC	0 TO 197	197 TO 225	225 TO 240	240 TO 250	250 TO 270	270 TO 280	280 TO 293	293 TO 305	305 TO END
$\Delta V_I/\Delta\phi$	-105.4	-27.2	-32.1	-40.1	-35.5	-20.3	-14.3	-1.8	0
$\Delta ASM/\Delta\phi$	.60	.15	.16	.16	0	0	0	0	0

MINIMUM FLIGHT PATH ANGLE

$\Delta V_I/\Delta\gamma_I = -3.85$ E3 M/S/DEG $\Delta ASM/\Delta\gamma_I = -24$ $M/sec^2/DEG$

TIME,SEC	0 TO 197	197 TO 225	225 TO 240	240 TO 250	250 TO 270	270 TO 280	280 TO 293	293 TO 305	305 TO END
$\Delta V_I/\Delta\phi$	-51.3	-.76	-.32	-.26	0	0	0	0	0
$\Delta ASM/\Delta\phi$	.31	0	0	0	0	0	0	0	0

LARGE VEHICLE 2

L/D	C_L	C_D	M/C_DA
.5	1	2	1147

MAXIMUM FLIGHT PATH ANGLE

$\Delta V_I/\Delta\gamma_I = 1.0$ E4 M/S/DEG $\Delta ASM/\Delta\gamma_I = -132$ $M/sec^2/DEG$

TIME,SEC	0 TO 197	197 TO 225	225 TO 240	240 TO 250	250 TO 270	270 TO 280	280 TO 293	293 TO 305	305 TO END
$\Delta V_I/\Delta\phi$	-20.1	-4.6	-13.3	-16.2	-14.1	-7.8	-5.3	.56	0
$\Delta ASM/\Delta\phi$	.1	0	0	0	0	0	0	0	0

MINIMUM FLIGHT PATH ANGLE

$\Delta V_I/\Delta\gamma_I = 930$ E3 M/S/DEG $\Delta ASM/\Delta\gamma_I = -33.7$ $M/sec^2/DEG$

TIME,SEC	0 TO 197	197 TO 225	225 TO 240	240 TO 250	250 TO 270	270 TO 280	280 TO 293	293 TO 305	305 TO END
$\Delta V_I/\Delta\phi$	-.1	-.44	-.03	0	0	0	0	0	0
$\Delta ASM/\Delta\phi$	0	0	0	0	0	0	0	0	0

TABLE 6 BANK ANGLES FOR TWO VEHICLES USING ATMOSPHERE 2

SMALL VEHICLE 2

L/D	C_L	C_D	M/C_DA
1	2	2	1000

MAXIMUM FLIGHT PATH ANGLE

$hp_1 = 38.9$ nm $hp_2 = 60.6$ nm $\gamma_I = -18.13$ deg

TIME	0 TO 197	197 TO 225	225 TO 240	240 TO 250	250 TO 270	270 TO 280	280 TO 293	293 TO 305	305 TO END
φ, deg	192	185	92	94	84	69	65	189	180

MINIMUM FLIGHT PATH ANGLE

$hp_1 = 32.4$ nm $hp_2 = 34.2$ nm $\gamma_I = -19.91$ deg

TIME	0 TO 197	197 TO 225	225 TO 240	240 TO 250	250 TO 270	270 TO 280	280 TO 293	293 TO 305	305 TO END
φ, deg	52	274	81	71	63	60	60	181	180

LARGE VEHICLE 2

L/D	C_L	C_D	M/C_DA
1	2	2	1147

MAXIMUM FLIGHT PATH ANGLE

$hp_1 = 39.5$ nm $hp_2 = 59.8$ nm $\gamma_I = -18.15$ deg

TIME	0 TO 197	197 TO 225	225 TO 240	240 TO 250	250 TO 270	270 TO 280	280 TO 293	293 TO 305	305 TO END
φ, deg	193.4	187	98	102	91	73	68	193	180

MINIMUM FLIGHT PATH ANGLE

$hp_1 = 29.1$ nm $hp_2 = 26.5$ nm $\gamma_I = -20.38$ deg

TIME	0 TO 197	197 TO 225	225 TO 240	240 TO 250	250 TO 270	270 TO 280	280 TO 293	293 TO 305	305 TO END
φ, deg	50	277	71	65	61	60	60	181	180

TABLE 7 SENSITIVITIES TO VARIATION IN INITIAL FLIGHT PATH ANGLE AND BANK ANGLE FOR ATMOSPHERE 2

SMALL VEHICLE 2

L/D	C_L	C_D	M/C_DA
1	2	2	1000

MAXIMUM FLIGHT PATH ANGLE

$\Delta V_I/\Delta\gamma_I$ = 1.0 E4 M/S/DEG　　$\Delta ASM/\Delta\gamma_I$ = -182 M/sec^2/DEG

TIME,SEC	0 TO 197	197 TO 225	225 TO 240	240 TO 250	250 TO 270	270 TO 280	280 TO 293	293 TO 305	305 TO END
$\Delta V_I/\Delta\phi$	-2.21	-3.91	-29.8	-40.7	-35.6	-19.0	-13.0	-2.14	0
$\Delta ASM/\Delta\phi$	0	0	.14	.12	0	0	0	0	0

MINIMUM FLIGHT PATH ANGLE

$\Delta V_I/\Delta\gamma_I$ = -200 E3 M/S/DEG　　$\Delta ASM/\Delta\gamma_I$ = -26 M/sec^2/DEG

TIME,SEC	0 TO 197	197 TO 225	225 TO 240	240 TO 250	250 TO 270	270 TO 280	280 TO 293	293 TO 305	305 TO END
$\Delta V_I/\Delta\phi$	-33.8	-.27	-.1	0	0	0	0	0	0
$\Delta ASM/\Delta\phi$	.32	0	0	0	0	0	0	0	0

LARGE VEHICLE 2

L/D	C_L	C_D	M/C_DA
1	2	2	1147

MAXIMUM FLIGHT PATH ANGLE

$\Delta V_I/\Delta\gamma_I$ = -1.59 E4 M/S/DEG　　$\Delta ASM/\Delta\gamma_I$ = -157 M/sec^2/DEG

TIME,SEC	0 TO 197	197 TO 225	225 TO 240	240 TO 250	250 TO 270	270 TO 280	280 TO 293	293 TO 305	305 TO END
$\Delta V_I/\Delta\phi$	-2.2	-5.9	-49.8	-69.2	-63.2	-35.0	-24.5	-4.0	0
$\Delta ASM/\Delta\phi$	0	0	.12	.10	0	0	0	0	0

MINIMUM FLIGHT PATH ANGLE

$\Delta V_I/\Delta\gamma_I$ = 688 E3 M/S/DEG　　$\Delta ASM/\Delta\gamma_I$ = -25.9 M/sec^2/DEG

TIME,SEC	0 TO 197	197 TO 225	225 TO 240	240 TO 250	250 TO 270	270 TO 280	280 TO 293	293 TO 305	305 TO END
$\Delta V_I/\Delta\phi$	-35.7	0	-1.3	0	0	0	0	0	0
$\Delta ASM/\Delta\phi$	.36	0	0	0	0	0	0	0	0

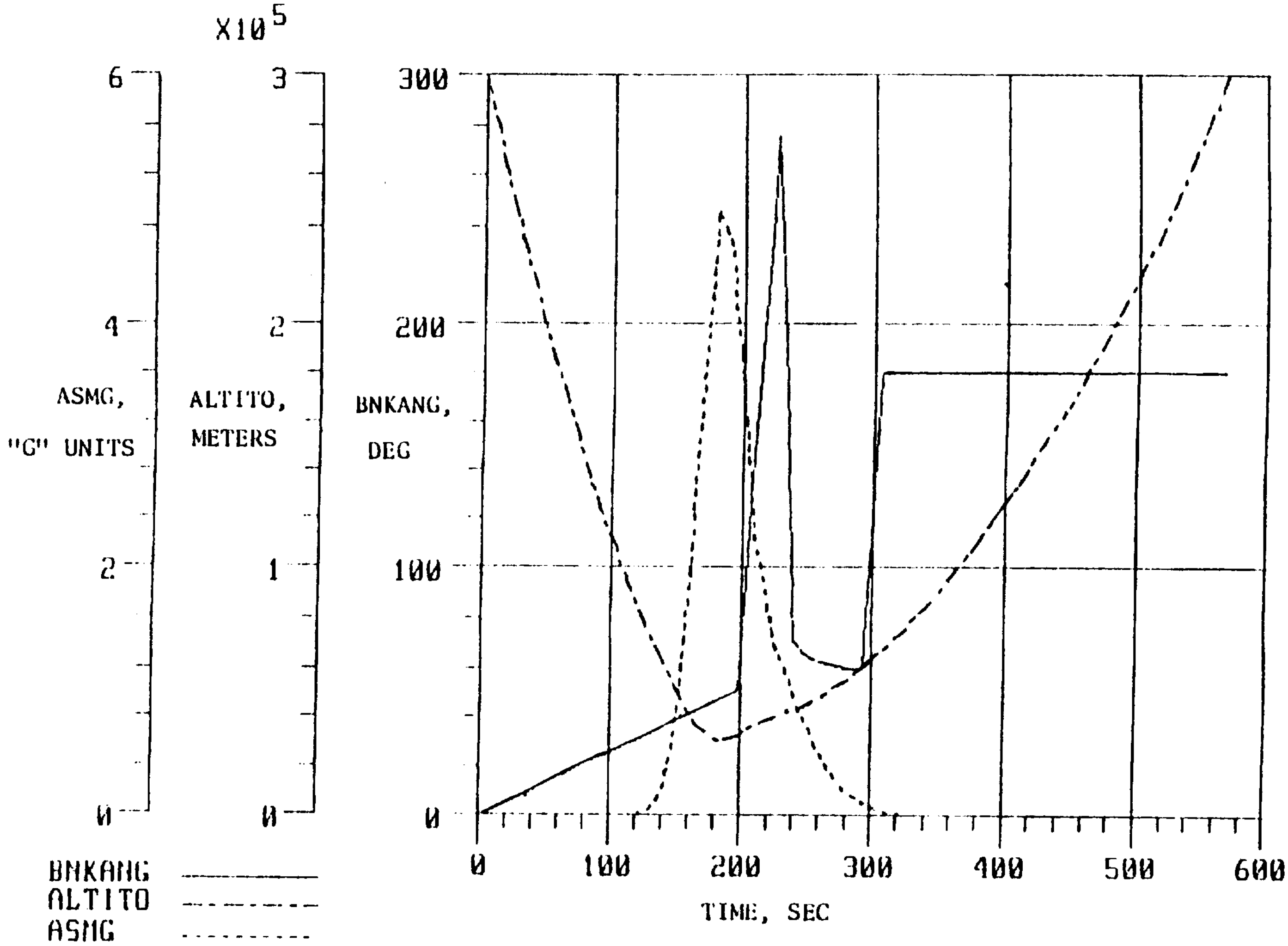

(a) Large Vehicle 2

$M/C_DA = 1147 \quad L/D = 1$

Figure 1. Time Histories of Bankangle, Altitude, and Acceleration for a Minimum Flight Path Angle Martian Entry.

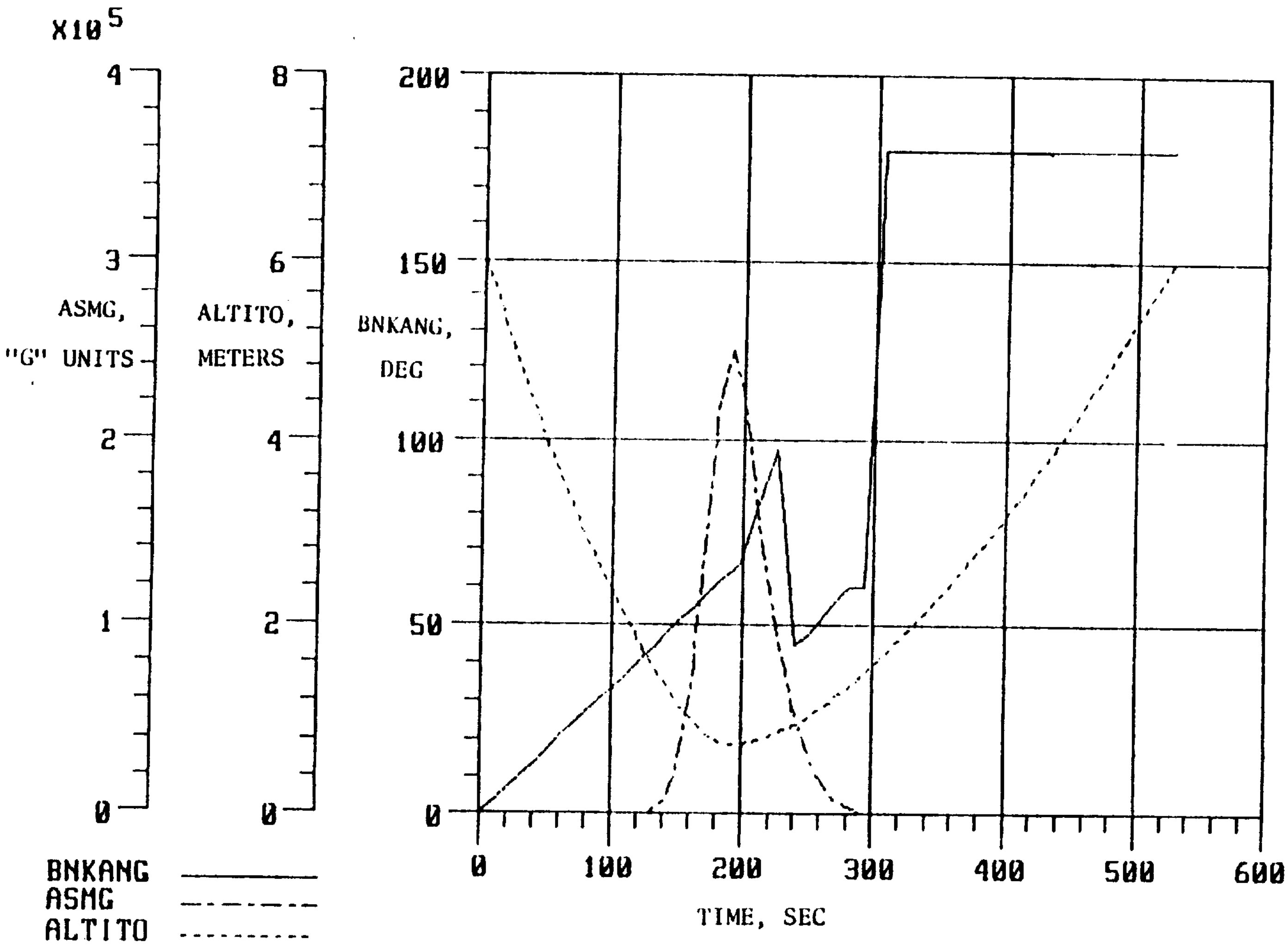

(b) Large Vehicle 1

$M/C_DA = 622 \quad L/D = 1.0$

Figure 1. Continued

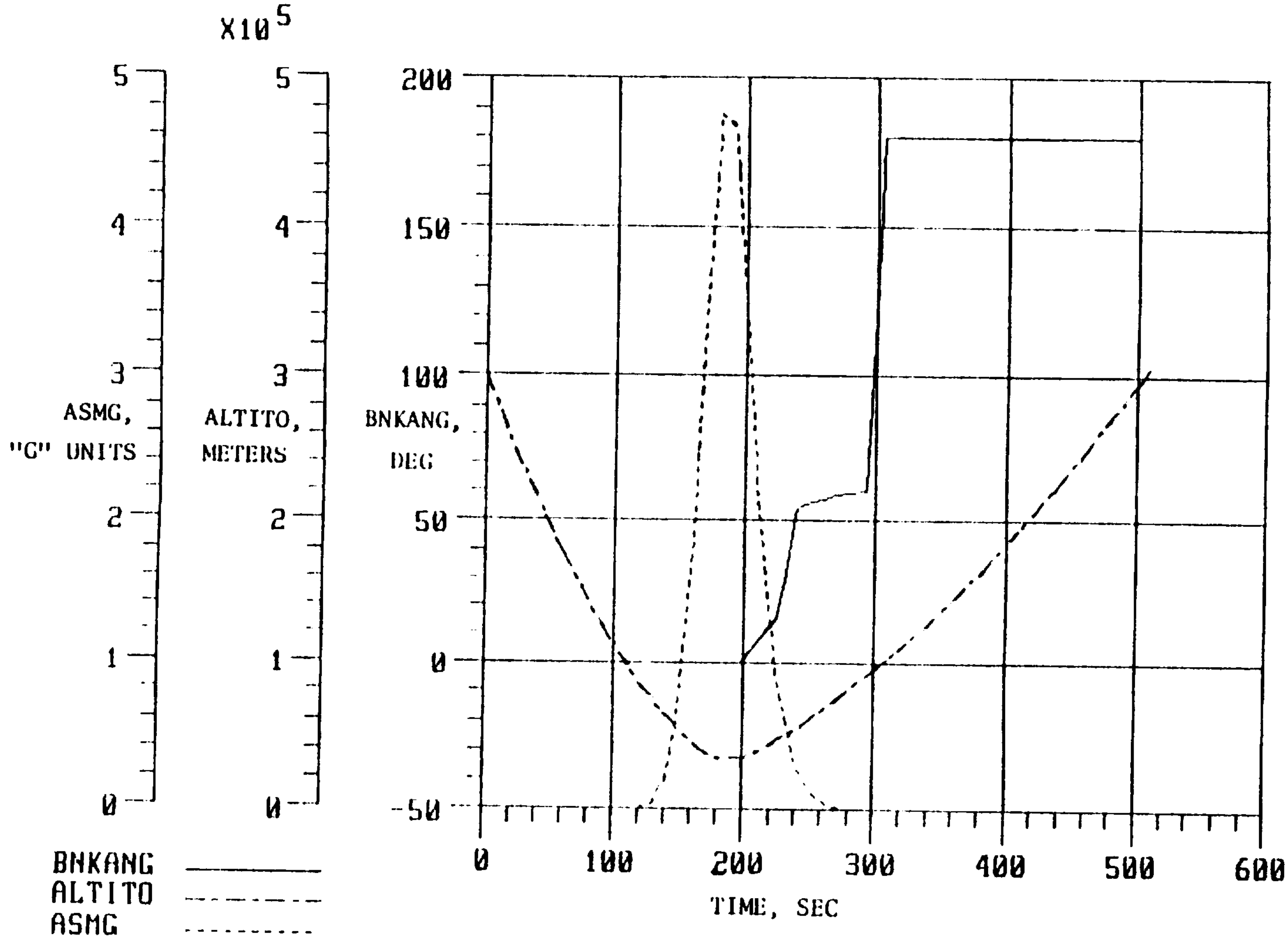

(c) Large Vehicle 1

$M/C_DA = 622$ $L/D = .5$

Figure 1. Concluded

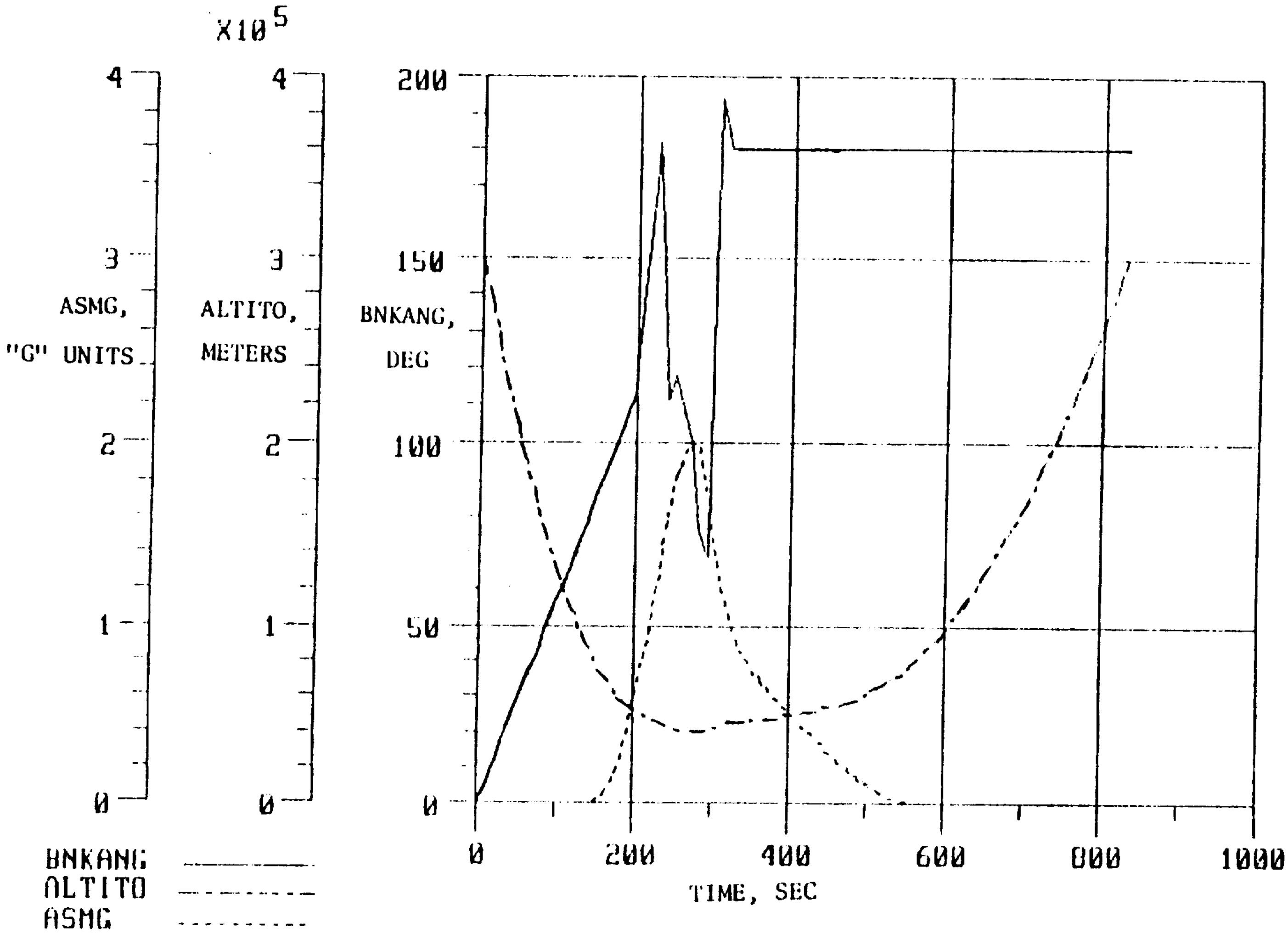

(a) Large Vehicle 2

$M/C_DA = 1147$ $L/D = 1$

Figure 2. Time Histories for Bankangle, Altitude, and Accleration for a Maximum Flight Path Angle Martian Entry.

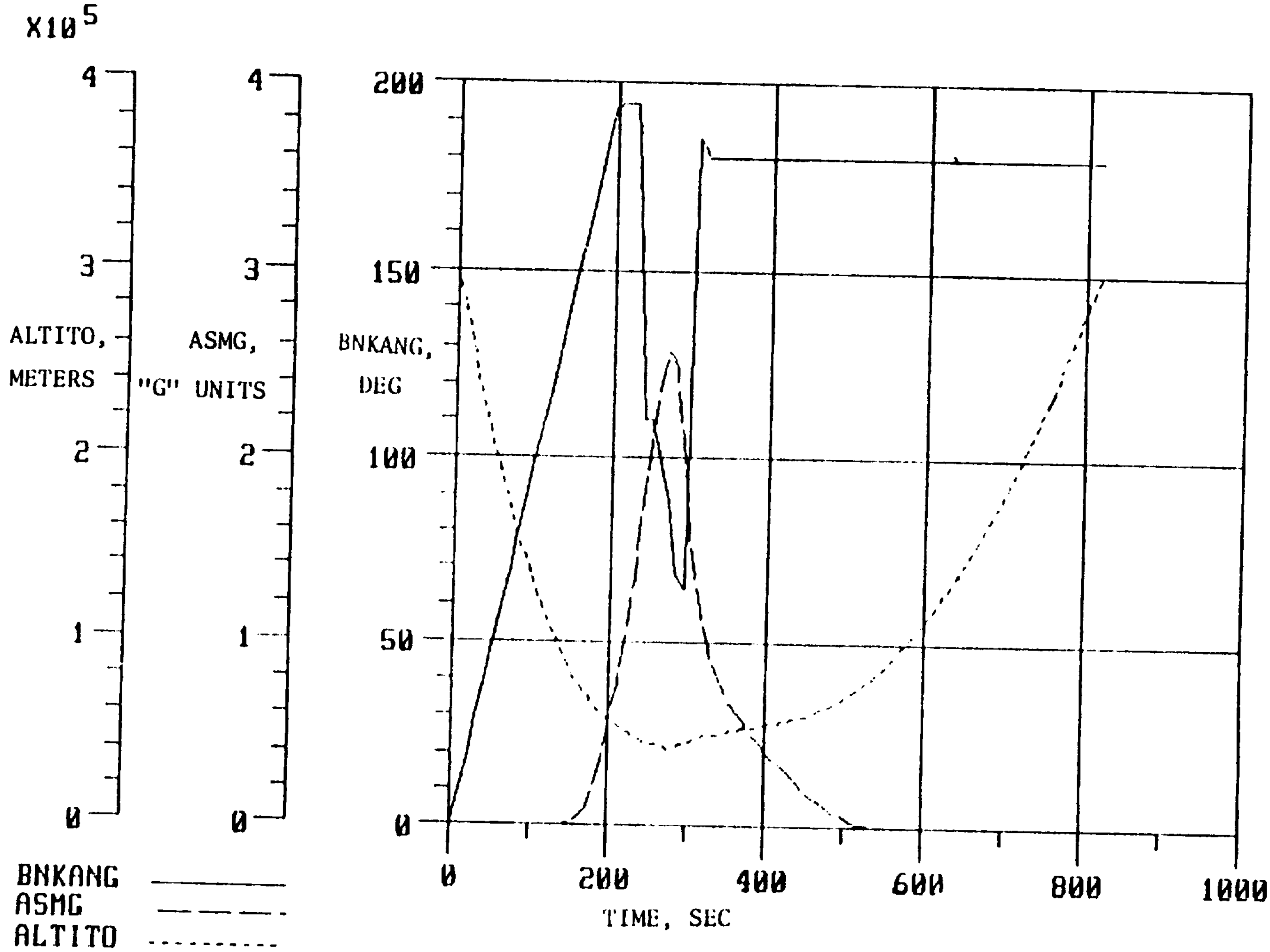

(b) Large Vehicle 1

$M/C_D A = 622$, $L/D = 1$

Figure 2. Continued

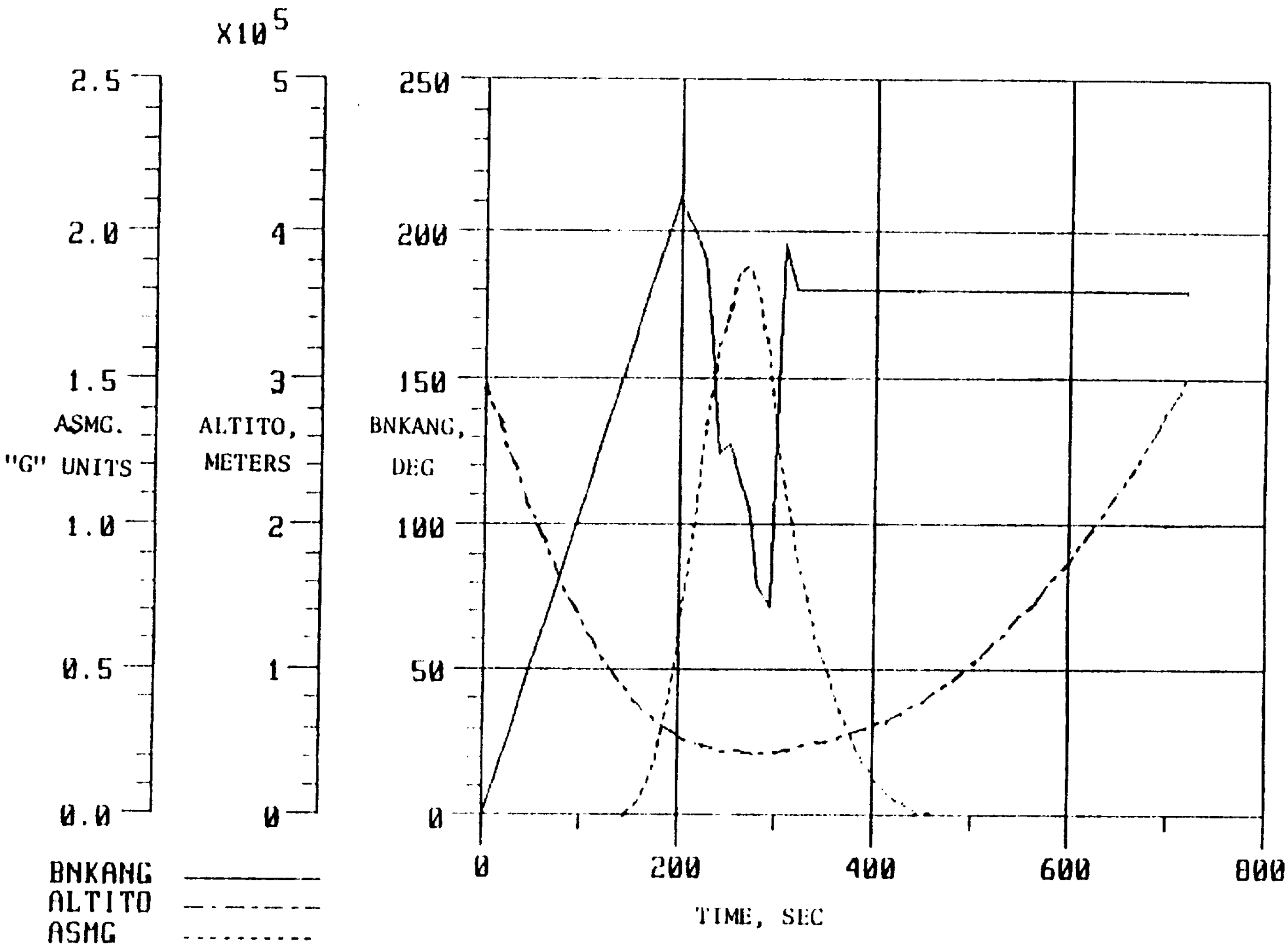

(c) Large Vehicle 1

M/C_DA = 622   L/D = .5

Figure 2. Concluded

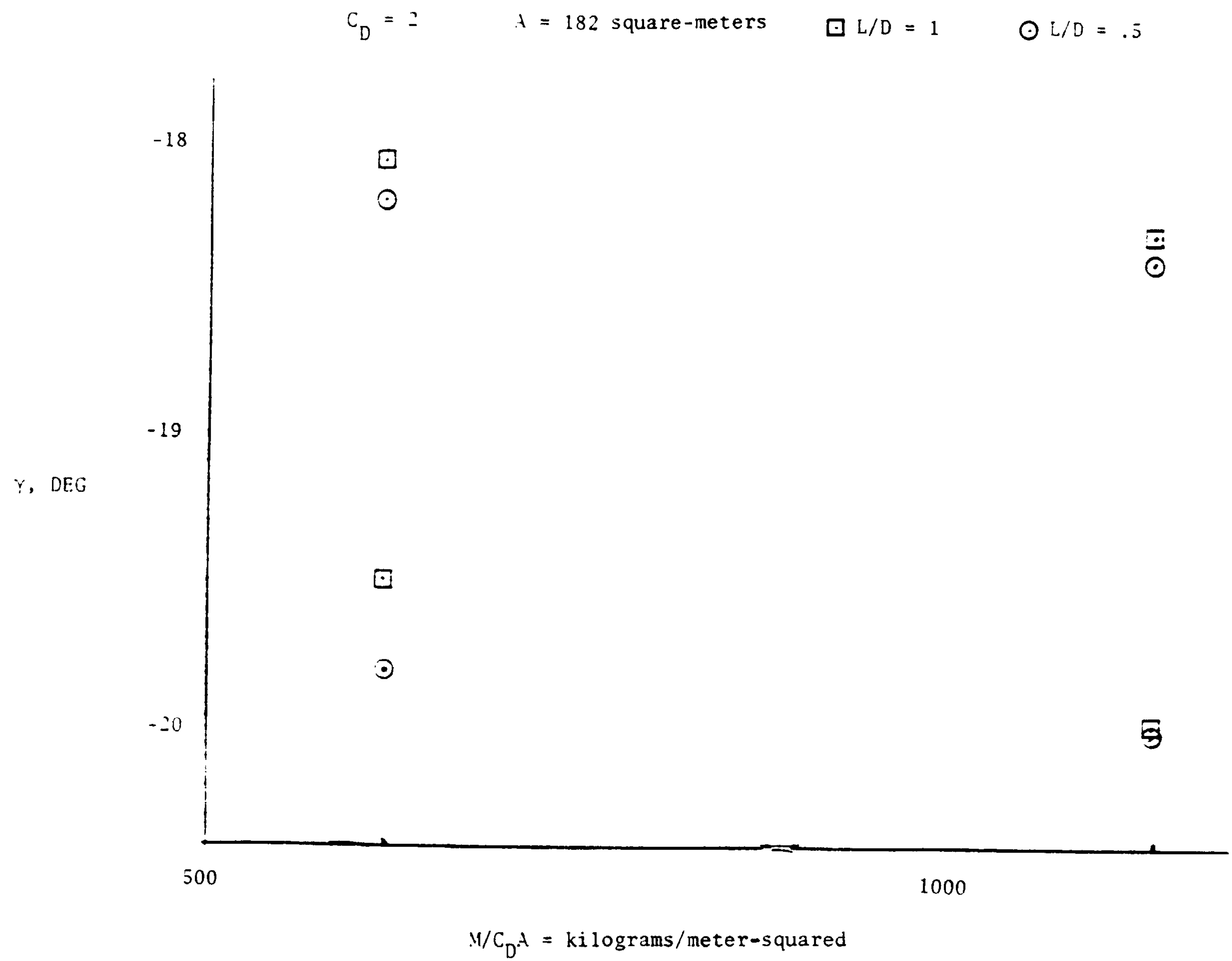

Figure 3. Entry Flight Path Angles for Various Entry Vehicles.

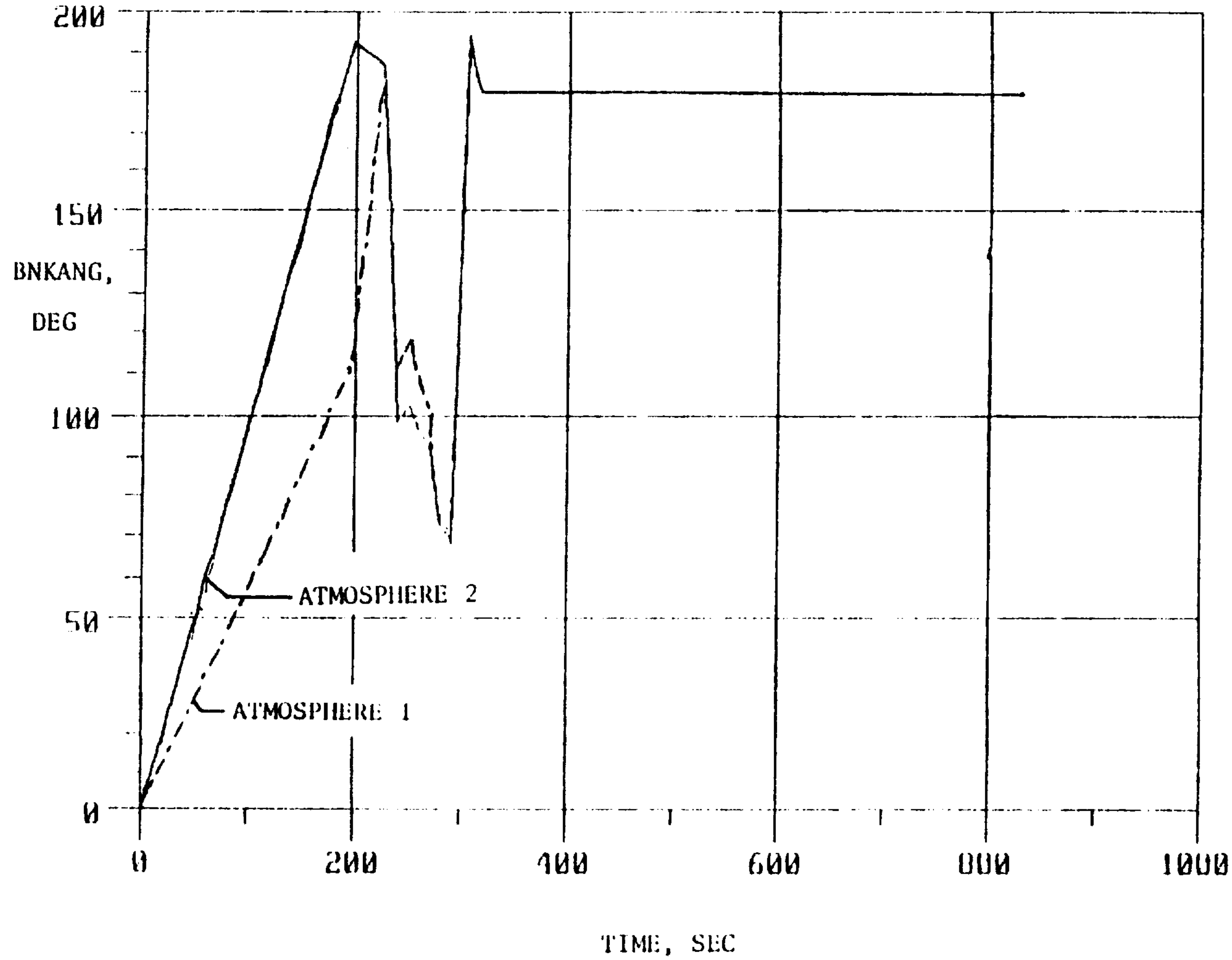

(a) Bankangle

Figure 4. Time Histories of Mars Entry for a Vehicle with L/D = 1 and $M/C_DA = 1147$ (Large Vehicle 2) using two atmospheric models.

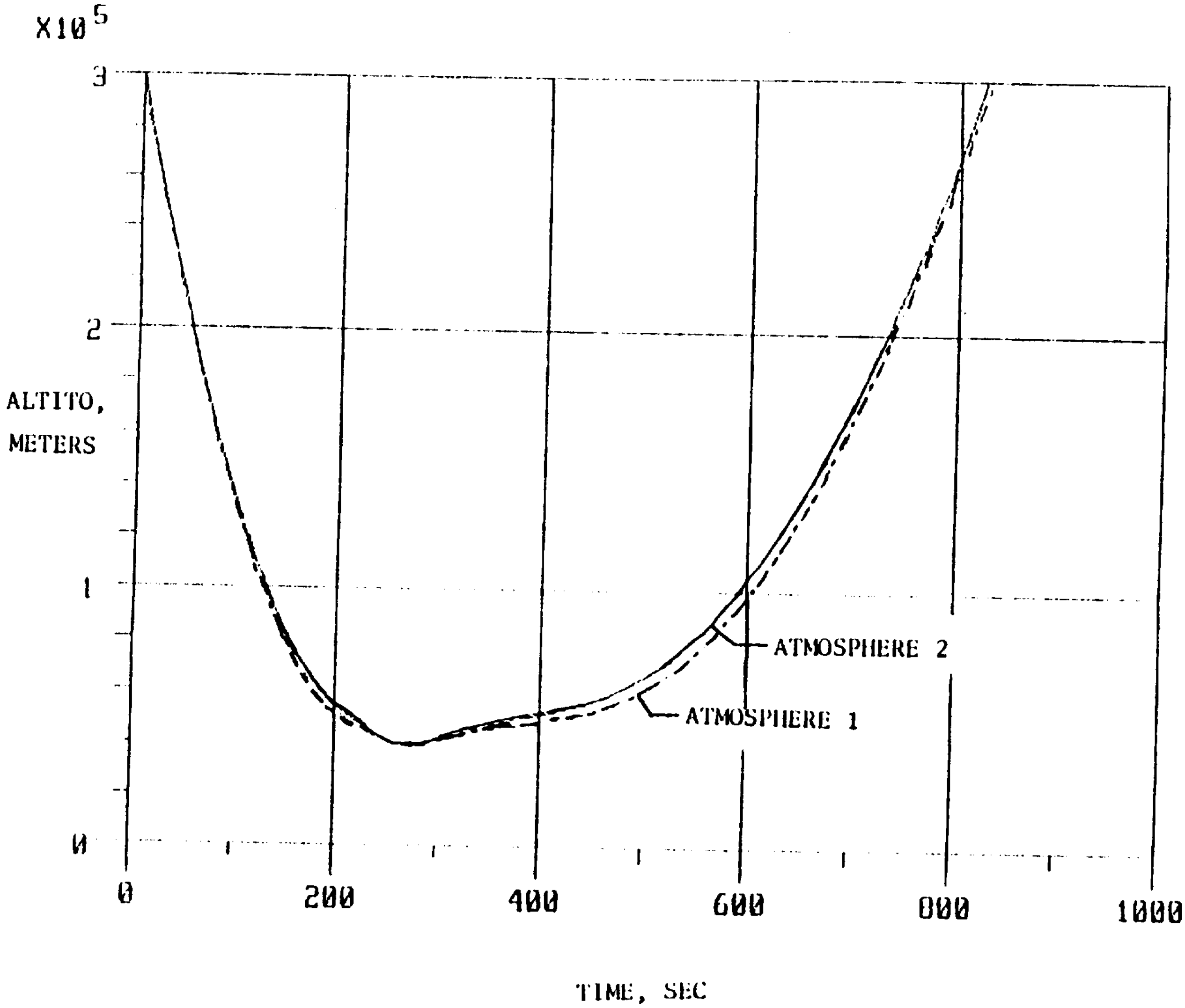

(b) Altitude

Figure 4. Continued

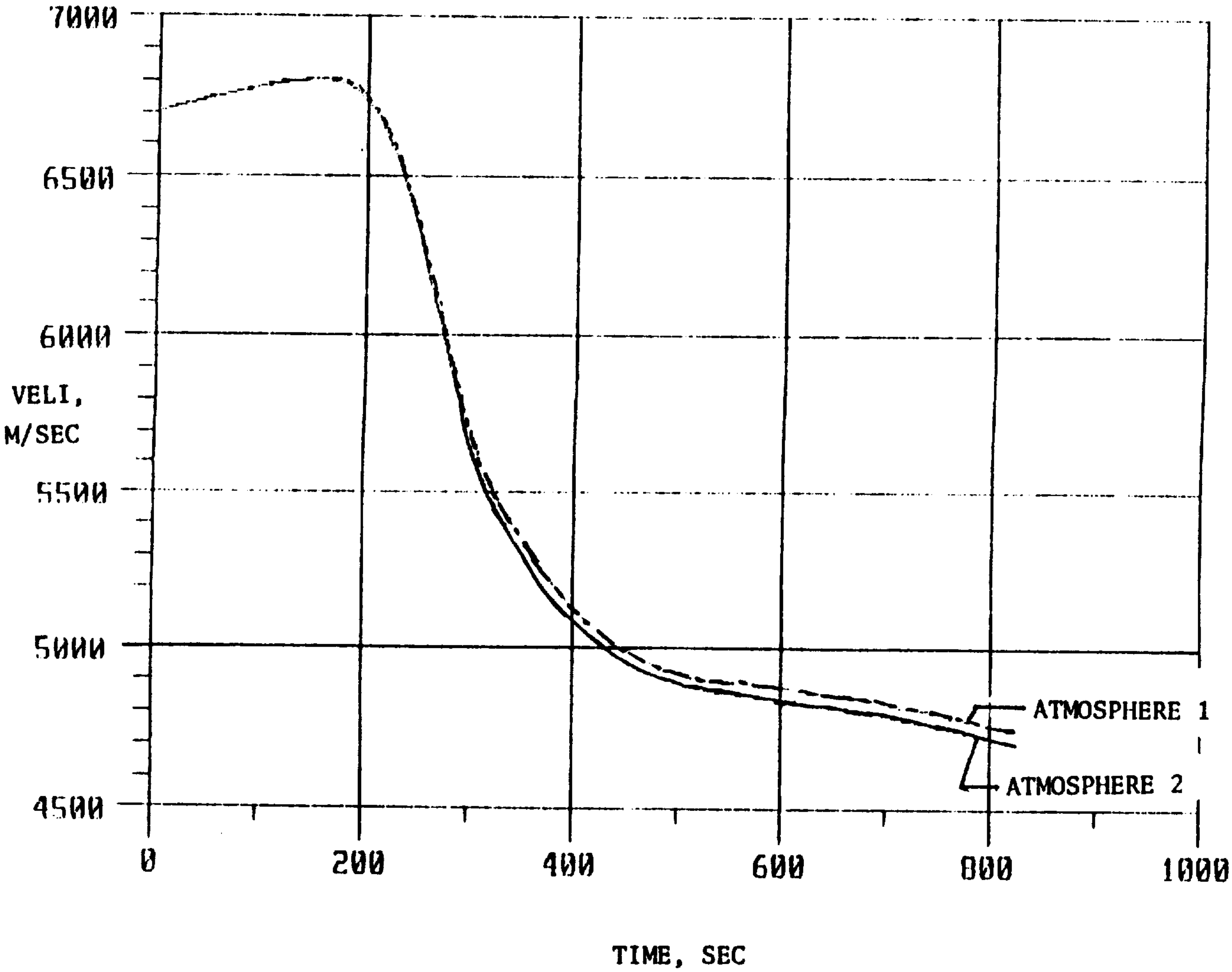

(c) Velocity

Figure 4. Concluded

NASA
National Aeronautics and Space Administration

Report Documentation Page

1. Report No. NASA TM-101607	2. Government Accession No.	3. Recipient's Catalog No.
4. Title and Subtitle Preliminary Investigation of Parameter Sensitivities for Atmospheric Entry and Aerobraking at Mars		5. Report Date September 1989
		6. Performing Organization Code
7. Author(s) Mary C. Lee and William T. Suit		8. Performing Organization Report No.
9. Performing Organization Name and Address NASA Langley Research Center Hampton, VA 23665-5225		10. Work Unit No. 506-46-21-01
		11. Contract or Grant No.
12. Sponsoring Agency Name and Address National Aeronautics and Space Administration Washington, DC 20546-0001		13. Type of Report and Period Covered Technical Memorandum
		14. Sponsoring Agency Code
15. Supplementary Notes		

16. Abstract

The proposed manned Mars mission will need to be as weight efficient as possible. This paper will discuss one way of lowering the weight of the vehicle by using aeroassist braking instead of retro-rockets to slow a craft once it reaches its destination. The two vehicles studied are a small vehicle similar in size to the Mars Rover Sample Return (MRSR) vehicle and a larger vehicle similar in size to a six-person Manned Mars Mission (MMM) vehicle. Simulated entries were made using various coefficients of lift (C_L), coefficients of drag (C_D), and lift-to-drag ratios (L/D). A range of acceptable flight path angles with their corresponding bank angle profiles was found for each case studied. These ranges were then compared, and the results are reported here. The sensitivity of velocity and acceleration to changes in flight path angle and bank angle is also included to indicate potential problem areas for guidance and navigation system design.

17. Key Words (Suggested by Author(s)) Spacecraft Guidance Aeroassist Spacecraft Maneuvers Manned Mars Mission	18. Distribution Statement Unclassified - Unlimited Subject Category 18

19. Security Classif. (of this report)	20. Security Classif. (of this page)	21. No. of pages	22. Price
Unclassified	Unclassified	29	A03